iomac
International Operational Modal Analysis Conference
11th International Operational Modal Analysis Conference
20 - 23 May 2025 | Rennes, France

Measuring displacements and vibration frequencies of wind towers by means of a ground-based radar interferometer

Giovanni Nico[1], *and Olimpia Masci*[2]

[1] Italy's National Research Council, Institute for Applied Mathematics "Mauro Picone", Bari, Italy
[2] DIAN S.r.l., Matera, Italy

ABSTRACT

The aim of this work is to study the application of Ground-Based Radar (GBR) interferometry technique to study the vibration characteristics of wind towers by remote acquisitions without the installation of any sensor or corner reflector on the monitored tower. In particular, the objective of this work is to demonstrate that it is possible to use the vibration frequency and amplitude measured by the GBR along the whole tower to discriminate the vibration behaviour of the tower in the cases of wind turbine at rest and in function. In addition, it will be shown that it is also possible to point out the differences in the vibration behaviour of two nearby wind towers, either in their oscillation frequency or amplitude. The methodology that is applied relies on the radar interferometry technique. A stack of Real Aperture Radar (RAR) profiles are collected providing the radar scattered signal for each target along the range directions. The amplitude of radar signal in each profile allows to identify the location of the wind tower. For each range pixel associated to the wind tower, the stack of range profiles is further processed to estimate the interferometric phase changes along the time and finally the temporal profile of displacements. The spectrum of each temporal profile is computed to identify the vibration frequencies. The results of an experiment carried out at a wind farm to study the differences in the vibration behaviour of two nearby wind towers are presented.

Keywords: Wind turbine, Vibro-diagnostics, Ground-based radar interferometer

1. INTRODUCTION

1.1. General information

Nowadays wind plants are an important source of green energy. Many wind turbines have been installed in windy regions. Usually, a wind turbine is dismissed after a certain number of years depending on the statistical assessment of its average productive life. However, the wind turbine health and productivity

depends on many factors, such as the position within the wind plant array and the proper installation. For this reason, the measurement of wind turbine displacements and vibration frequencies, both when active and at rest, is important to assess the proper turbine functioning. Ground-based Radar (GBR) sensors have been proposed for the monitoring of wind plants, in synergy with terrestrial laser scanner [1]. An overview of the application of GBR sensors for the monitoring of infrastructures is given in [2]. An application of GBR technique to the monitoring of pier is reported in [3]. It is worth pointing out the applications of monitoring of bridges (e.g. [4], [5], [6]) and telecommunication towers [7] that are examples of infrastructures having geometrical and functional characteristics similar to the case study of wind towers. In this work we present the results which have been obtained by measuring the wind displacements and vibration frequencies by means of the ground based radar interferometry technique. Measurements have been acquired using a Ku-band radar which has been installed at different locations around the wind turbine to avoid any blind position where the main component of the displacement vector is perpendicular to the radar Line-of-Sight (LoS). A methodology to display the displacements of the whole wind turbines directly in the field has been developed. The time series of displacements, as the well as the corresponding spectrum of vibration frequencies, are estimated for all the structural elements of wind turbines with a range resolution of 0.75 m. The stack of vibration spectra is used as a tool for a quick inspection of the vibration behaviour. In addition, a procedure for the geolocation of ground-based measurements is presented, needed for both the rendering of radar measurements over the wind tower and to correlate it to the wind direction at the time of radar acquisitions. The methodology presented in this work, based on the in-situ radar measurements, has been applied for the real-time assessment of vibrational behaviour of wind towers, without interrupting turbine operations. The stack of vibration spectra provided by ground-based radar measurements could provide a means to quickly detect excessive vibrations in the field. The manuscript is organized as follows. Section 2 describes the methodology for collect the process GBR data. Results. are presented in section 3 and discussed in section 4. Finally, a few conclusions are drawn in section 5.

2. METHODOLOGY

The methodology used in this experiments consists of following steps: 1) measurements of key acquisition parameters in the field, i.e. elevation angle, distance of the GBR with respect to the basis of the wind tower, vertical and horizontal angular width of the -3dB main beam of antennas; 2) focusing of GBR radar data to get a stack of Single-Look-Complex (SLC) radar range profiles, each with a range resolution of 0.75m, and a time stamp; 3) interferometric processing of the SLC radar data to get a time series of interferometric phase values, i.e. the temporal changes of SLC phase values; 4) estimation of the time series of LoS displacement and 5) spectral analysis of each time series of LoS displacement to identify the vibration frequencies. Steps 3) to 5) are applied to each range pixel of the SLC radar range profiles, separately. Figure 1 shows the radar configuration geometry. The elevation angle ϑ and distance d from the wind tower are reported. The angle α denotes the vertical angular width of the antenna's main lobe (i.e. the 3dB lobe). It depends on the antennas used for data acquisition. The angles α and ϑ, as well as the distance d should be set carefully to be sure that the whole wind tower is observed by the radar. The height of the whole wind tower is denoted by L, while h is the height of the lower part of the tower. The range distance D between the GBR and each target on the wind tower is compute as

$$D = d \tan \vartheta \tag{1}$$

Eq. (1) is used to compute the range distances D_1 and D_2 of the lower and upper targets corresponding to the -3dB main lobe.

$$\begin{cases} D_1 = d \tan\left(\vartheta - \dfrac{\alpha}{2}\right) \\ D_2 = d \tan\left(\vartheta + \dfrac{\alpha}{2}\right) \end{cases} \tag{2}$$

The difference between the two range distances D_1 and D_2 has to be be larger than the height L of the whole wind tower. In addition, the elevation angle should set in such a way that $D_1 \sim d$ to observe the wind tower from its basis.

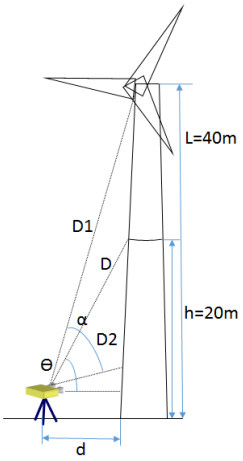

Figure 1. Acquisition geometry of GBR data.

3. RESULTS

The GBR measurements have been collected at two nearby towers of the same wind farm. The two wind towers are denoted a N. 86 and N. 89. The GBR sensor has been installed at a distance $d = 140\ m$ from the wind tower N. 86 and $d = 60\ m$ from the wind tower N. 89. The elevation angle of was set to $\vartheta = 15$ and $25°$. Two further acquisitions have been collected at the wind tower N. 86 setting $\vartheta = 10°$. Table 1 and Table 2 summarize the values of elevation angle, the status of the wind turbine and the wind speed and direction during the acquisition of GBR data.

Table 1. Summary of GBR acquisitions at wind tower N. 86.

Elevation angle ϑ [deg]	Status of the wind turbine	Time, wind speed and direction
25	In function	13:40 9,8 m/s W 13:45 8,9 m/s W 13:50 8,5 m/s W
25	At rest	13:55 9,8 m/s W 14:00 8,8 m/s W 14:05 9,7 m/s W
15	At rest	14:10 11,2 m/s W 14:15 10,7 m/s W 14:20 12,1 m/s W
15	In function	14:25 12,1 m/s W 14:30 11,9 m/s W 14:35 11,4 m/s W 14:40 10,2 m/s W
10	In function	14:45 10,3 m/s W 14:50 10,8 m/s W 14:55 8,9 m/s W 15:00 9,1 m/s W
10	At rest	15:05 8,5 m/s W 15:10 10,5 m/s W 15:15 11,3 m/s W

Table 2. Summary of GBR acquisitions at wind tower N. 89.

Elevation angle ϑ [deg]	Status of the wind turbine	Time, wind speed and direction
25	In function	13:40 9,8 m/s W 13:45 8,9 m/s W 13:50 8,5 m/s W
25	At rest	13:55 9,8 m/s W 14:00 8,8 m/s W 14:05 9,7 m/s W
15	At rest	14:10 11,2 m/s W 14:15 10,7 m/s W 14:20 12,1 m/s W
15	In function	14:25 12,1 m/s W 14:30 11,9 m/s W 14:35 11,4 m/s W 14:40 10,2 m/s W

Figure 2 displays the results obtained at the wind tower N. 86 with the wind turbine in function and a rest. Each acquisition last 15 minutes. Analogously, **Figure 3** to **Figure 8** display the results obtained at the wind tower N. 89 with the wind turbine in function and a rest, for different structural of the tower.

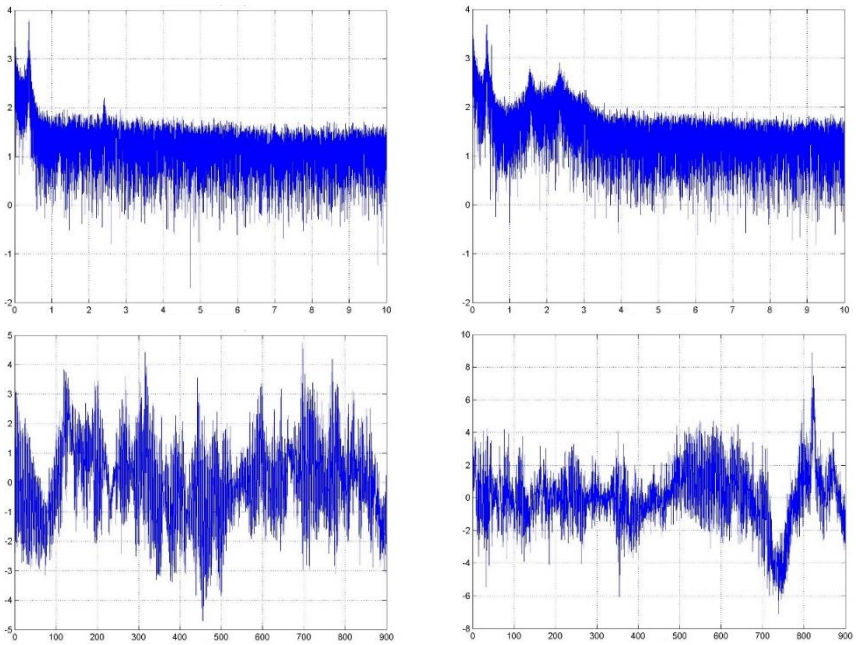

Figure 2. Measurements at the wind tower N. 86. (left) wind turbine at rest. (right) wind turbine in function. Top: Frequency spectrum vs. frequency. Bottom: amplitude in [mm] vs. time [s].

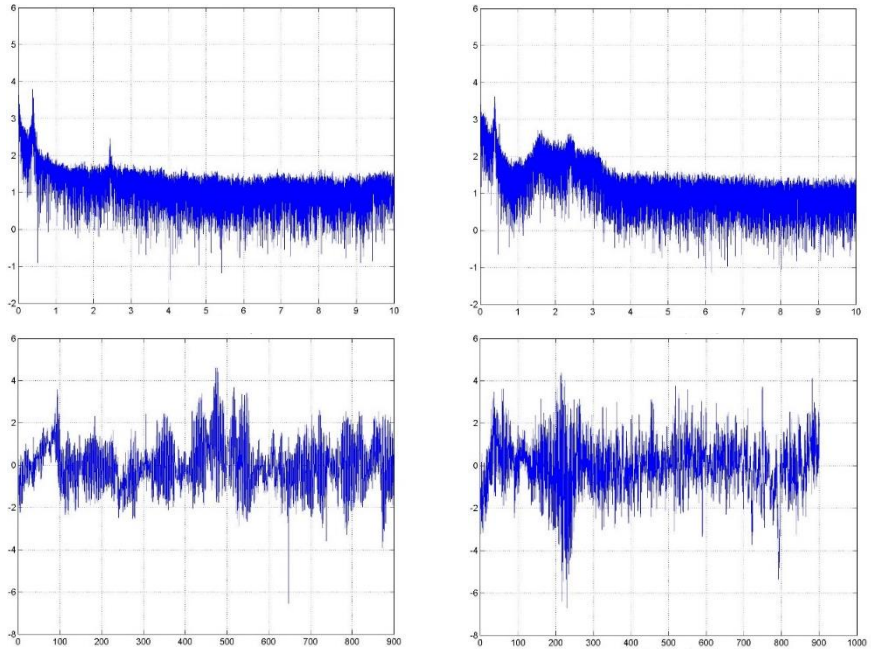

Figure 3. Measurements at the wind tower N. 89. (left) wind turbine at rest. (right) wind turbine in function. Top: Frequency spectrum vs. frequency. Bottom: amplitude in [mm] vs. time [s]. Measurements are referred to the segment of the wind tower located at $H = 15\ m$ above the ground.

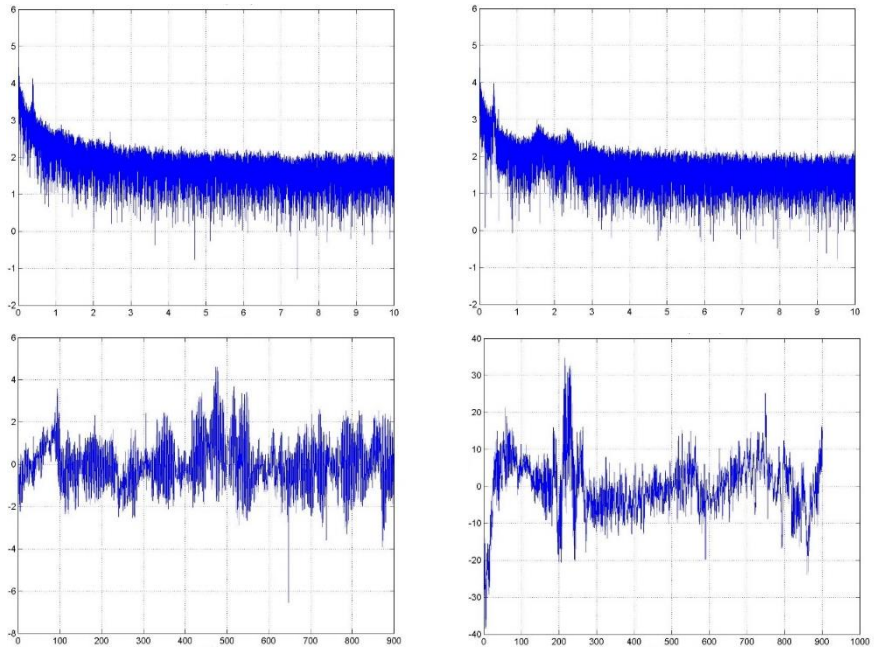

Figure 4. Measurements at the wind tower N. 89. (left) wind turbine at rest. (right) wind turbine in function. Top: Frequency spectrum vs. frequency. Bottom: amplitude in [mm] vs. time [s]. Measurements are referred to the segment of the wind tower located at $H = 24\ m$ above the ground.

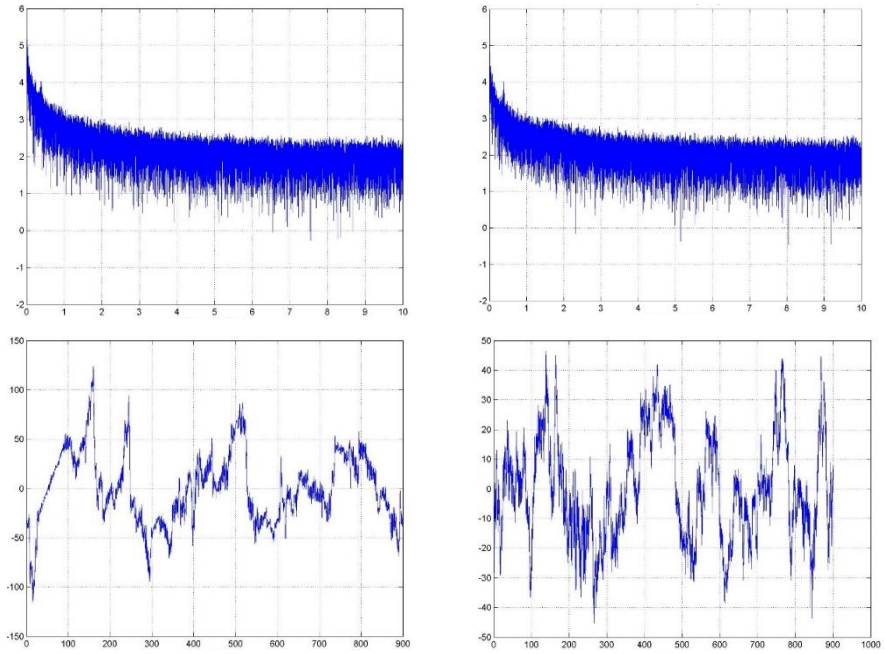

Figure 5. Measurements at the wind tower N. 89. (left) wind turbine at rest. (right) wind turbine in function. Top: Frequency spectrum vs. frequency. Bottom: amplitude in [mm] vs. time [s]. Measurements are referred to the segment of the wind tower located at *H = 29 m* above the ground.

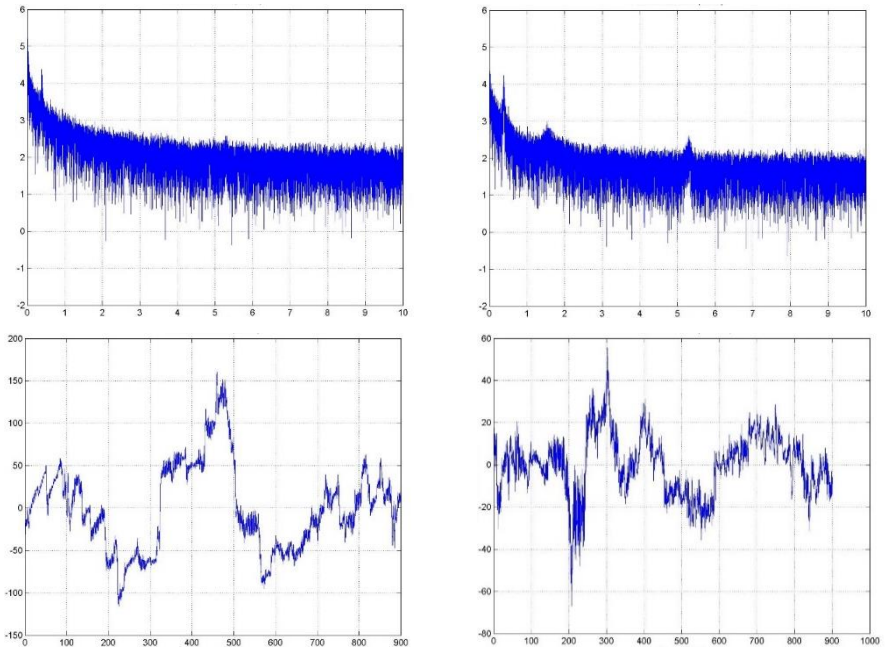

Figure 6. Measurements at the wind tower N. 89. (left) wind turbine at rest. (right) wind turbine in function. Top: Frequency spectrum vs. frequency. Bottom: amplitude in [mm] vs. time [s]. Measurements are referred to the segment of the wind tower located at *H = 34 m* above the ground.

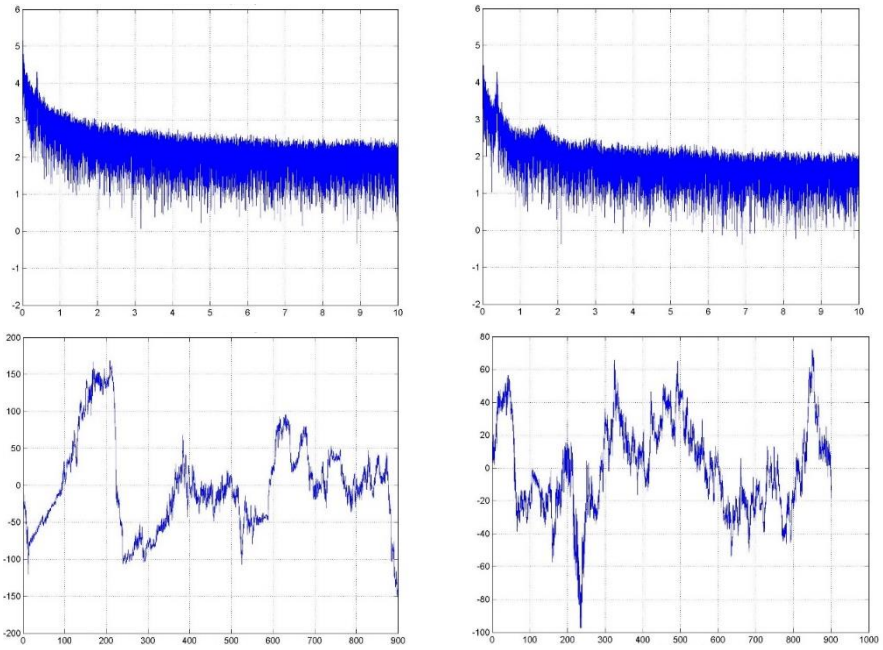

Figure 7. Measurements at the wind tower N. 89. (left) wind turbine at rest. (right) wind turbine in function. Top: Frequency spectrum vs. frequency. Bottom: amplitude in [mm] vs. time [s]. Measurements are referred to the segment of the wind tower located at *H = 37 m* above the ground.

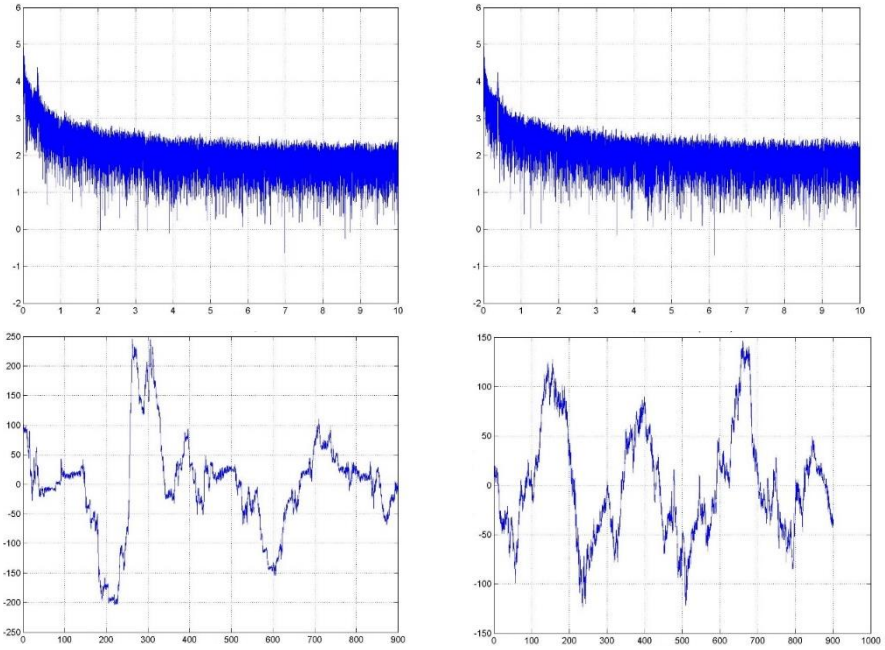

Figure 8. Measurements at the wind tower N. 89. (left) wind turbine at rest. (right) wind turbine in function. Top: Frequency spectrum vs. frequency. Bottom: amplitude in [mm] vs. time [s]. Measurements are referred to the segment of the wind tower located at *H = 42 m* above the ground.

4. DISCUSSION

This work focused on the comparison of vibration characteristics of two wind towers located at the same wind farm. In-situ have been collected within a time interval of less than two hours in similar wind and weather conditions. The acquisition and processing of GBR data has been done following a procedure that allows to identify the vibration amplitude and frequency of different segment of towers

with a range resolution of *0.75 m*. It has been found that wind towers 86 and 89 have similar vibration characteristics in terms of oscillation amplitude and vibration frequency up to a height of about *20 m* with respect to the ground. However, in the upper part of the wind turbine N. 89 have been measured vibrations with a peak-peak oscillation amplitude of *45 cm*. In particular, this maximum amplitude of *45 cm* has been measured in the case of non-operating wind turbine while in the case of wind turbine in function it has been measured a vibration with a peak-to-peak amplitude of *30 cm*. A similar behavior has been observed along the whole upper part of the wind tower, about a height of twenty-nine meters, even if with a decreasing peak-to-peak amplitude from to the top to lower heights. We could provide two interpretations to the measured vibrations amplitude in the upper part of wind tower N. 89. The first interpretation is based on the turbine rotation around the tower axis, due to the rotation of blades. This causes a change in the radar acquisition geometry which has been set at the beginning of data acquisition in order in increase the LoS component of the turbine oscillation amplitude. However, if the movement of blades causes a rotation of the wind turbine during the data acquisition, the GBR measures a smaller LoS and, as a consequence, underestimate the amplitude of the turbine oscillation. It is worth noting that the rotation of wind turbine does not affect the estimate of the vibration frequency. A second interpretation of the measured amplitudes is related to the "stabilizing effect" of turbine movement which could induce an oscillatory movement having a smaller amplitude with respect to the case of a wind turbine at rest.

5. CONCLUSIONS

In this work the GBR interferometer has been used to compare the frequency and amplitude measurements of wind tower oscillations. It has been found that it is possible to discriminate the vibration behaviour of structural elements of a wind tower and of two different wind towers of the same wind farm. Furthermore, the changes of vibration amplitude and frequency of the same wind tower when the wind turbine is in operation or at rest have also been detected. As a future work, the impact of averaging vibration spectra on the estimation accuracy of vibration frequencies will be investigated. Radar data of the wind tower, in the same working condition, have to be collected at different times during the same measurement session. In addition, it will be studied a methodology to identify modal parameters of wind towers in GBR vibration spectra.

REFERENCES

[1] S. Artese and G. Nico. TLS and GB-RAR measurements of vibration frequencies and oscillation amplitudes of tall structures: An application to wind towers. *Applied Sciences*, 10(7), 2237, 2022.

[2] A. Anghel, M. Tudos, R. Cacoveanu, M. Datcu, G. Nico, O. Masci, A. Dongyang, W. Tian, C. Hu, Z. Ding, H. Nies, O. Loffeld, D. Atencia, S.G. Huaman, A. Medella, J. Moreira. Compact ground-based interferometric synthetic aperture radar: short-range structural monitoring. *IEEE Signal Processing Magazine*, 36(4), 42-52, 2019.

[3] G. Nico, G. Cifarelli, G. Miccoli, F. Soccodato, W. Feng, M. Sato, S. Miliziano, M. Marini. Measurement of pier deformation patterns by ground-based SAR interferometry: application to a bollard pull trial. *IEEE Journal on Oceanic Engineering*, 43(4), 822-829, 2018.

[4] M. Pieraccini, M. Fratini, F. Parrini, G. Macaluso, and C. Atzeni, High-speed CW step-frequency coherent radar for dynamic monitoring of civil engineering structures, *Electronic Letters*, 40, 907, 2004.

[5] L. Zou, W. Feng, O. Masci, G. Nico, A.M. Alani, M. Sato. Bridge monitoring strategies for sustainable development with microwave radar interferometry. *Sustainability*, 16(7), 2607, 2024.

[6] L. Zou, G. Nico, A.M. Alani, M. Sato. Strategy for vertical deformation of railway bridge monitoring using polarimetric ground-based real aperture radar system. Structural Health Monitoring, 14, 14759217231226128, 2024.

[7] G. Nico, G. Prezioso, O. Masci, and S. Artese, Dynamic modal identification of telecommunication towers using ground based radar interferometry, *Remote Sensing*, 12(7), 1211, 2020.